Structural determination of Si(100)2×2-Al by tensor LEED

H. Sakama, K. Murakami, K. Nishikata, and A. Kawazu
Department of Applied Physics, The University of Tokyo, 7-3-1 Hongo, Bunkyo-ku, Tokyo 113, Japan
(Received 11 February 1993; revised manuscript received 2 June 1993)

The structure of a Si(100)2×2-Al surface at 0.5 monolayers is determined by tensor low-energy electron diffraction. The parallel dimer model is more favorable than the orthogonal dimer model. The *R* factor for the optimized parallel dimer structure is 0.15. The bond length of the Al dimer is almost equal to the value expected from the Pauling covalent radii. All bond lengths in five surface layers including Si-Al and Si dimer bonds are within the range of 5% from the bulk value. The distortion extends at least through the first five layers into the bulk.

I. INTRODUCTION

Al-adsorbed Si(100) surfaces were investigated by several researchers with low-energy electron diffraction (LEED) and scanning tunneling microscopy (STM).[1–5] It was demonstrated that a well-defined 2×2 phase is formed at 0.5 monolayers (ML's) (where 1 ML corresponds to 9.6×10^{14} atoms/cm^2). Here, $2\times n$ ($n=3,5,7$) phases where the 2× periodicity of the clean Si(100) 2×1 surface along the dimer is maintained emerge. Knall *et al.* proposed the model of the local atomic arrangement of 2×2 on the indium-adsorbed Si(100) surface.[6] They concluded that two indium atoms form a dimer similar to the Si dimer on the Si(100) 2×1 surface. In their model, the indium dimer is orthogonal to the Si dimer (ortho dimer) underneath.

On the other hand, Nogami and co-workers observed one-dimensional dimer rows of Al, Ga, and In lying between Si dimer rows, using STM.[3–5] One bright spot was clearly observed between the Si dimer in the empty-state image. They attributed it to the ad dimer of Al, Ga, and In consistent with the model proposed by Knall *et al.* The saturation coverage where these one-dimensional rows entirely cover the surface was estimated at 0.5 ML. Recently, Northrup *et al.* performed first-principles total-energy calculations on the 2×2 surface and concluded that the configuration of the ad dimer which is parallel to the Si dimer (para dimer) is favorable in comparison with that of the ortho dimer.[7] They also found that the surface-state dispersion calculated for the 2×2 indium para-dimer structure is in good agreement with the angle-resolved photoemission data. However, there is still room for further study with regard to the detailed atomic arrangement of the 2×2 structure.

The aim of this work is to determine the atomic arrangement of Si(100)2×2-Al with tensor LEED.

II. EXPERIMENTAL DETAILS

The experiments are performed in a standard ultrahigh-vacuum chamber equipped with four-grid LEED optics. Other experimental details concerning the preparation of Al-adsorbed surfaces are described in Ref. 2. A fast LEED system to measure the intensity versus voltage (*I-V*) curves of diffracted beams consists of a highly sensitive TV camera, a large-volume memory, and a magneto-optical disk controlled by a microcomputer.[8]

The intensities of the beams are measured with the normal incidence of an electron. The 2×2 LEED pattern is proven to have 4-mm symmetry from the *I-V* curves of diffracted beams. Mirror planes are (0,1,−1) and (0,1,1). The spectra of the *I-V* curves of the symmetric beams are almost identical. However, their intensities and/or the relative heights of the peaks sometimes deviate from one to another due to the slightly off-normal incident angle of the electrons. *I-V* curves are averaged among symmetric beams to obtain one representative *I-V* curve. This treatment effectively cancels the above effect. Moreover, it reduces noises which arise from the background of the LEED pattern. The latter factor is especially essential for the improvement of *I-V* curves of high index beams because the primary signal-to-noise ratio is small due to the weak intensities. Consequently, 12 independent *I-V* curves become available for the structure analysis. The LEED pattern and the beams used in the calculation are illustrated in Fig. 1.

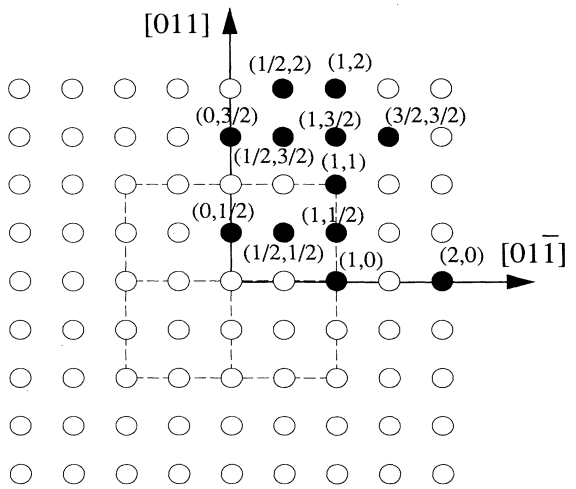

FIG. 1. A schematic diagram of the LEED pattern from the Si(100)2×2-Al surface. Open circles denote diffraction spots. Filled circles denote 12 beams used in the analysis. Four of them are the integral-order beams and the rest are the fractional-order beams. Dashed lines represent reciprocal unit cells of the Si(100) surface.

III. RESULTS AND DISCUSSION

The atomic arrangements of parallel- (para) and orthogonal- (ortho) dimer models are shown in Fig. 2. The geometrical parameters are defined in Fig. 2. Both models satisfy 2-mm symmetry, while they are lacking in fourfold-rotational symmetry. The latter feature contradicts the 4-mm symmetry observed in the Al-induced 2×2 pattern. The 2×2 pattern is composed of two subpatterns. The contributions from these two subpatterns to the 2×2 pattern are always the same. One of these subpatterns (the first subpattern) originates from the domain where Si dimers are oriented parallel to the y axis as defined in Fig. 2. The other one (the second subpattern) is from the domain where Si dimers are oriented parallel to the x axis. Thus, the second subpattern is obtained by 90° rotation from the first one, giving rise to the fourfold-rotational symmetry of the observed 2×2 pattern. The fourfold-rotational symmetric beam in the first subpattern is always superposed on each beam of the first subpattern in the 2×2 pattern. In the procedure of calculations, I-V curves of the first subpattern are initially evaluated on the basis of the geometrical models shown in Fig. 2. Then, I-V curves of the fourfold-rotational symmetric beam are added to the I-V curves of each beam to form one theoretical I-V curve of this beam.

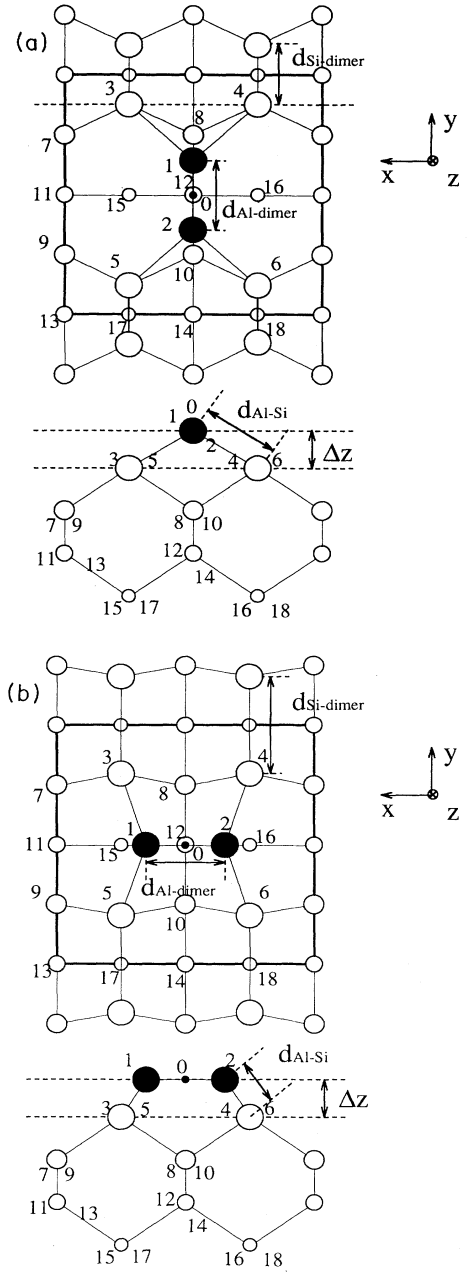

FIG. 2. The atomic arrangements of (a) para- and (b) ortho-dimer models. Open and filled circles denote Si and Al atoms, respectively. The size of the open circles indicates the layer number from the surface. Namely, the largest atoms are located in the topmost surface layer. All atoms are numbered from 1 to 18. Four parameters ($d_{Al\ dimer}$, $d_{Si\ dimer}$, $d_{Al\text{-}Si}$, and Δz) used for the definition of the geometry are shown by the arrows. Heavy and fine solid lines denote a unit cell of 2×2 and the chemical bonds between two atoms, respectively. Here, x, y, and z axes are defined as $[0,-1,1]$, $[0,1,1]$, and $[-1,0,0]$, respectively.

The amplitudes of diffracted beams are calculated using tensor LEED.[9,10] We use the program developed by Rous, Van Hove, and Somorjai.[11] The tensor LEED scheme consists of two steps.[12] In the first step, the amplitudes of beams for a reference structure are calculated by a conventional full dynamical method. In the second step, the deviation of the amplitude due to a small displacement from the reference structure is evaluated by first-order perturbation theory. The trial structure whose Pendry's R factor is the lowest is automatically found.[13] The displacements of 18 atoms within the first five surface layers are taken into consideration. The movement of each atom which breaks 2-mm symmetry is forbidden. For example, the movements of atoms 1 and 2 in Fig. 2 (Al-dimer atoms) along the y and z axes are allowed, while those along x are always forbidden. If atom 1 is displaced by Δy along the y axis, atom 2 is forced to be simultaneously displaced by $-\Delta y$. This rule is based on the assumption of symmetric Al dimers. The original program in Ref. 11 is modified because of this rule.

The validity of the perturbation in the second step of tensor LEED is thought to be restricted to within 0.4 Å from the reference structure in the case of the metal surface.[9] The limit is possibly as much as 0.2 Å in the present case because the shape of the I-V curves for the trial structure displaced more than 0.2 Å from the reference structure is found to be seriously distorted. The reference structures numerous enough to cover the entire parameter space must be considered at intervals of less than 0.4 Å for all parameters. The parameter range of the reference structures is listed in Table I. One

TABLE I. The parameter range of reference structures used in the calculation. All values are given in units of Å.

	Para dimer	Ortho dimer	Interval
$d_{Al\ dimer}$	2.30–2.90	2.30–2.80	0.1
$d_{Si\ dimer}$	2.30–2.80	2.30–2.90	0.1
$d_{Al\text{-}Si}$	2.30–2.80	2.30–2.90	0.1
Δz	1.00–1.20	0.60–1.00	0.1

definitive result is obtained corresponding to one reference structure. Among all results, the geometry with the minimum R factor is chosen as a final one in the first stage. Pendry's R factors for the geometries at this stage are 0.19 and 0.27 for the para- and ortho-dimer models, respectively. This finding indicates that the actual surface has the para-dimer structure.

Another calculation is required with the final geometry at the first stage as a reference structure for the precise determination of the atomic arrangement of the para-dimer model. The optimized geometry with the global minimum R factor is obtained after one cycle of tensor LEED. The R factor for the final geometry at the first stage slightly deteriorates to 0.22 by a full dynamical calculation in the first step of tensor LEED. The R factor for the optimized geometry after the second step of tensor LEED improves to 0.15. This optimized geometry is reliable because the displacement of each atom at this geometry from the reference structure is less than 0.05 Å. The experimental I-V curves and the theoretical ones optimized for both para- and ortho-dimer models are shown in Fig. 3. (I-V curves for the ortho-dimer model are those obtained at the first stage.) Geometrical parameters for the optimum geometries in para- and ortho-dimer models are shown in Table II. Two groups have reported the geometries so far using energy calculations.[7,14] Their results are also given in Table II in terms of the parameters defined in Fig. 2. In these cases, the structures of only the first two (Al dimer and Si dimer) layers are optimized. We also calculate I-V curves for their structures assuming that the atoms from the third-to-fifth layers keep their bulk positions. The R factors for the geometries of para- and ortho-dimer models given by Northrup *et al.* are estimated as 0.40 and 0.45, respectively. The R factor for Batra's geometry on the ortho-dimer model is 0.43.

The coordinates of 18 atoms in the optimum geometry on the para-dimer model are shown in Table III. The most remarkable feature of our result is that the bond length of the Al dimer is 2.50 Å, which is consistent with the expected value from the Pauling covalent radii of 2.52 Å. In contrast, the bond length of the Al dimer in the geometry proposed by Northrup is 2.69 Å as shown in Table II, which is longer by 7% than the above expected value. Concerning other parameters, our result is almost equivalent to that of Northrup *et al.* Both Al-Si and Si-dimer bond lengths are within the range of 5% from the sum of the Pauling covalent radii. In addition, all bond lengths of Si located below the second layer are within the range of 5% from the bulk value except for the length

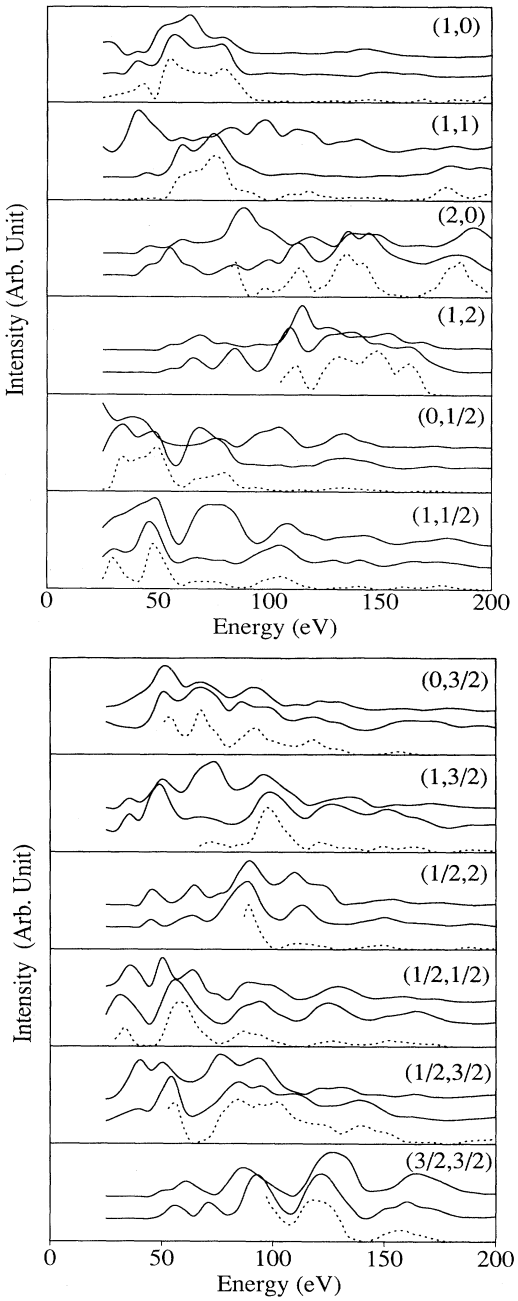

FIG. 3. Experimental (dashed line) and theoretical (solid line) I-V curves optimized for the para- and ortho-dimer model. Upper and lower solid lines correspond to the ortho- and para-dimer models, respectively.

TABLE II. Parameters of the optimized geometries in para- and ortho-dimer models. Each value is given in units of Å. The Si-dimer bond length was not defined in Ref. 14.

	This work (para dimer)	Northrup *et al.* (para dimer)	This work (ortho dimer)	Northrup *et al.* (ortho dimer)	Batra (ortho dimer)
Al dimer	2.50	2.69	2.51	2.58	2.57
Si dimer	2.44	2.44	2.35	2.69	None
Al-Si	2.50	2.47	2.88	2.67	2.81
Δz	1.08	1.10	0.72	0.71	0.74

TABLE III. The coordinates of 18 atoms in the optimized para-dimer model. They are given in units of Å. Three axes are defined in Fig. 2(a).

Atom no.	x	y	z
1	0.00	1.25	0.00
2	0.00	−1.25	0.00
3	1.80	2.62	1.08
4	−1.80	2.62	1.08
5	1.80	−2.62	1.08
6	−1.80	−2.62	1.08
7	3.84	1.84	2.22
8	0.00	1.87	2.60
9	3.84	−1.84	2.22
10	0.00	−1.87	2.60
11	3.84	0.00	3.43
12	0.00	0.00	4.08
13	3.84	−3.84	3.37
14	0.00	−3.84	4.00
15	2.08	0.00	4.95
16	−2.08	0.00	4.95
17	2.08	−3.84	5.17
18	−2.08	−3.84	5.17

between atoms 13 and 17 in Fig. 2. This rather large deviation from the bulk value seems to be derived from the insensitivity of the I-V curves to the displacement in deep layers.

The other feature of the geometry on the para-dimer model is that the distortion of surface layers extends at least to the first five layers into the bulk. Applebaum and Hamann also showed the evidence of atomic diplacements extending to five subsurface layers on a clean Si(100) 2×1 surface with Keating strain-energy minimization calculation.[15] In the present geometry, the Si dimer structure is also maintained. However, two Si dimers in a 2×2 unit cell approach the Al dimer by approximately 0.2 Å. Therefore, the adsorption of Al atoms induces an additional surface lattice strain. Subsurface layers are reconstructed to relax this strain, which results in the deeply extending distortion into the bulk.

IV. CONCLUSIONS

The atomic arrangement of the Si(100)2×2-Al surface is successfully determined by tensor LEED. In this geometry, the dimer of Al atoms is adsorbed parallel to the Si dimers on the Si(100) surface. The bond length of the Al dimer is almost equal to the value expected from the Pauling covalent radii. All bond lengths included in five surface layers are within the range of 5% from the bulk value, indicating that the proposed geometry is reliable. The distortion extends to, at least, the first five layers into the bulk.

ACKNOWLEDGMENTS

We wish to thank Dr. A. Wander and Dr. M. A. Van Hove of Lawrence Berkeley Laboratory for providing the programs and for helpful discussions. We also wish to thank N. Akiyama of Komatsu Electric Metals Co. for supplying the samples.

[1]T. Ide, T. Nishimori, and T. Ichinokawa, Surf. Sci. **209**, 335 (1989).
[2]K. Murakami, K. Nishikata, M. Yoshimura, and A. Kawazu, Appl. Surf. Sci. **60/61**, 146 (1992).
[3]A. A. Baski, J. Nogami, and C. F. Quate, J. Vac. Sci. Technol. A **8**, 245 (1990).
[4]J. Nogami, A. A. Baski, and C. F. Quate, Phys. Rev. B **44**, 1415 (1991).
[5]A. A. Baski, J. Nogami, and C. F. Quate, J. Vac. Sci. Technol. A **9**, 1946 (1991).
[6]J. Knall, J.-E. Sundgren, G. V. Hansson, and J. E. Greene, Surf. Sci. **166**, 512 (1986).
[7]J. E. Northrup, M. C. Schabel, C. J. Karlsson, and R. I. G. Uhrberg, Phys. Rev. B **44**, 13 799 (1991).
[8]K. Nishikata, K. Murakami, M. Yoshimura, and A. Kawazu, Surf. Sci. **269/270**, 995 (1992).
[9]P. J. Rous and J. B. Pendry, Surf. Sci. **219**, 355 (1989); **219**, 373 (1989).
[10]P. J. Rous, J. B. Pendry, D. K. Saldin, K. Heinz, K. Mueller, and N. Bickel, Phys. Rev. Lett. **57**, 2951 (1986).
[11]P. J. Rous, M. A. Van Hove, and G. A. Somorjai, Surf. Sci. **226**, 15 (1990).
[12]P. J. Rous and J. B. Pendry, Comput. Phys. Commun. **54**, 137 (1989); **54**, 157 (1989).
[13]J. B. Pendry, J. Phys. C **13**, 937 (1980).
[14]I. P. Batra, Phys. Rev. Lett. **63**, 1704 (1989).
[15]J. A. Appelbaum and D. R. Hamann, Surf. Sci. **74**, 21 (1978).